Article

The Role of the 5f Orbitals in Bonding, Aromaticity, and Reactivity of Planar Isocyclic and Heterocyclic Uranium Clusters

Athanassios C. Tsipis, Christos E. Kefalidis, and Constantinos A. Tsipis

More About This Article

Additional resources and features associated with this article are available within the HTML version:

- Supporting Information
- Access to high resolution figures
- Links to articles and content related to this article
- Copyright permission to reproduce figures and/or text from this article

View the Full Text HTML

The Role of the 5f Orbitals in Bonding, Aromaticity, and Reactivity of Planar Isocyclic and Heterocyclic Uranium Clusters

Athanassios C. Tsipis,[†] Christos E. Kefalidis,[‡] and Constantinos A. Tsipis*,[‡]

Laboratory of Inorganic and General Chemistry, Department of Chemistry, University of Ioannina, 451 10 Ioannina, Greece, and Laboratory of Applied Quantum Chemistry, Faculty of Chemistry, Aristotle University of Thessaloniki, 541 24 Thessaloniki, Greece

Received March 31, 2008; E-mail: tsipis@chem.auth.gr

Abstract: The molecular and electronic structures, stabilities, bonding features and magnetic properties of prototypical planar isocyclic *cyclo*-U_nX_n ($n = 3$, 4; X = O, NH) and heterocyclic *cyclo*-$U_n(\mu_2$-X$)_n$ ($n = 3$, 4; X = C, CH, NH) clusters as well as the $E@[c$-$U_4(\mu_2$-C$)_4]$, (E = H$^+$, C, Si, Ge) and $U@[c$-$U_5(\mu_2$-C$)_5]$ molecules including a planar tetracoordinate element E (ptE) and pentacoordinate U (ppU) at the ring centers, respectively, have been thoroughly investigated by means of electronic structure calculation methods at the DFT level. It was shown that 5f orbitals play a key role in the bonding of these f-block metal systems significantly contributing to the cyclic electron delocalization and the associated magnetic diatropic (magnetic aromaticity) response. The aromaticity of the perfectly planar *cyclo*-U_nX_n ($n = 3$, 4; X = O, NH), *cyclo*-$U_n(\mu_2$-X$)_n$ ($n = 3$, 4; X = C, CH, NH), $E@[c$-$U_4(\mu_2$-C$)_4]$, (E = H$^+$, C, Si, Ge) and $U@[c$-$U_5(\mu_2$-C$)_5]$ clusters was verified by an efficient and simple criterion in probing the aromaticity/antiaromaticity of a molecule, that of the nucleus-independent chemical shift, NICS(0), NICS(1), NICS$_{zz}$(0) and the most refined NICS$_{zz}$(1) index in conjunction with the NICS scan profiles. Natural bond orbital analyses provided a clear picture of the bonding pattern in the planar isocyclic and heterocyclic uranium clusters and revealed the features that stabilize the ptE's inside the six- and eight-member uranacycle rings. The ptE's benefit from a considerable electron transfer from the surrounding uranium atoms in the $E@[c$-$U_4(\mu_2$-C$)_4]$, (E = H$^+$, C, Si, Ge) and $U@[c$-$U_5(\mu_2$-C$)_5]$ clusters justifying the high occupancy of the np orbitals of the central atom E.

Introduction

There has been a recent resurgence of interest in understanding the electronic structure of 5f-block element compounds.[1] This is driven principally by the desire to predict the behavior of actinide species in a variety of applications, from waste repositories to the design of selective chemical separation methodologies. Noteworthy is the recently reported unique bonding pattern in the U_2 diatomic molecule that corresponds to a quintuple bond involving three electron-pair bonds and four one-electron bonds.[2] The role of the 5f orbitals in bonding and reactivity is still one of the most intriguing questions in actinide chemistry and continues to be a topic of considerable debate among theoretical and experimental chemists. The high nodality of the 5f orbitals and the expended electron count of binary organoactinide clusters provide the opportunity for the actinide metals to engage in peculiar bonding schemes that are not available to the d-block elements, leading to new patterns of reactivity. The chemistry of the actinide elements represents a challenging yet vital scientific frontier, and its development requires fundamental understanding of the relative roles of actinide valence region orbitals and the nature of their chemical bonding. Accurate theoretical description of the actinide ele-

ments and their compounds is one of the grand challenge areas for modern computational quantum chemistry. Besides fundamental interest there is a strong incentive for the theoretical study of actinide complexes and clusters providing useful data to augment and enhance the otherwise extreme experimental difficulties arising from the radioactivity of the actinide elements. However, because of the very many electrons that have to be dealt with, the scalar relativistic and correlation effects along with the comparatively close in energy and spatial extent of the 5f, 6d, 7s, and 6p orbitals, allowing all of them to participate in bonding, the calculations become cumbersome, with problems in achieving convergence in the self-consistent solution of the quantum mechanical equations. Motivated by the peculiar chemical bonding mechanism and the versatile reactivity of actinide molecules as well as by the stunning growth of the aromaticity concept in "all-metal" aromatic rings[3–5] we were challenged to explore the role of the 5f orbitals in bonding,

† University of Ioannina.
‡ Aristotle University of Thessaloniki.
(1) Evans, W. J. *Inorg. Chem.* **2007**, *46*, 3435.
(2) Gagliardi, L.; Roos, B. O. *Nature* **2005**, *433*, 848.

(3) (a) Li, X. A.; Kuznetsov, E.; Zhang, H. F.; Boldyrev, A. I.; Wang, L. S. *Science* **2001**, *291*, 859–861. (b) Boldyrev, A. I.; Wang, L. S. *Chem. Rev.* **2005**, *105*, 3716.
(4) (a) Tsipis, C. A.; Tsipis, A. C. *J. Am. Chem. Soc.* **2003**, *125*, 1136. (b) Tsipis, C. A.; Karagiannis, E. E.; Kladou, P. F.; Tsipis, A. C. *J. Am. Chem. Soc.* **2004**, *126*, 12916. (c) Tsipis, C. A.; Tsipis, A. C. *J. Am. Chem. Soc.* **2005**, *127*, 10623. (d) Tsipis, C. A. *Coord. Chem. Rev.* **2005**, *249*, 2740. (e) Tsipis, A. C.; Stalikas, A. V. *New J. Chem.* **2007**, *31*, 852.
(5) Wannere, C. S.; Corminboeuf, C.; Wang, Z.-X.; Wodrich, M. D.; King, R. B.; Schleyer, P. v. R. *J. Am. Chem. Soc.* **2005**, *127*, 5701.

Table 1. The Spectroscopic Parameters of Small-Sized Uranium Species Computed at the BP86/SDD(U)∪6-31G(d,p)(X) (X = Nonmetal Element) Level

molecule	state	E_{tot} (hartrees)	R (U-E) (Å)	frequencies (cm^{-1})	IE (eV)
U	^5L	−51.536766			5.699 (6.1841 ± 0.0005)[a]
U$^+$	^4I	−51.327310			
UO	^5I	−126.839172	1.865 (1.8383 ± 0.0006)[a]	785.7 (846.5)[a]	5.961 (6.0313 ± 0.0006)[a]
UO$^+$	^4I	−126.620091	1.822 (1.802)[b]	842.6 (912)[b]	
US	$^5H/^5\Pi$	−449.821691	2.446 (2.378)[c]	376.5 (451.1)[c]	6.987
US$^+$	$^4H/^4\Pi$	−449.564917	2.348	458.6	
UC	quintet	−89.484576	1.964	565.2	6.183
UC$^+$	$^2\Delta$	−89.257344	2.342	459.2	
U(NH)	quintet	−106.905907	1.958	732.2	5.811
U(NH)$^+$	quartet	−106.692333	1.924	734.8	
CUO	$^5A'$	−164.807491	C−U = 2.046 U−O = 1.854	618.9 771.5	
CUO	$^3\Phi$	−164.803342	C−U = 1.904 (1.857)[d] U−O = 1.839 (1.825)[d]	605.9 (828)[d] 803.3 (893)[d]	
CUO	$^1\Sigma^+$	−164.769539	C−U = 1.804 (1.773)[e] U−O = 1.820 (1.808)[e]	882.0 (1062)[f] 792.6 (881)[f]	
NUO	$^2\Phi$	−181.592746	N−U = 1.735 (1.748)[f] U−O = 1.811 (1.837)[f]	1000.2 (1005)[g] 835.0 (834)[g]	7.858
NUO$^+$	$^1A'$	−181.297406	N−U = 1.696 (1.695) U−O = 1.755 (1.746)[e]	1079.9 (1081)[e] 944.7 (942)[e]	
NUN	$^1\Sigma^+$	−161.024030	1.732 (1.734)[e]	1013.9 (999) 1056.5 (1064) [1077][g,e]	8.738
NUN$^+$	$^4A'$	−160.702892	1.793	858.6; 926.2	
U$_2^{2+}$	singlet	−102.300082	2.130 (2.30)[h]	294.8	
U$_2^{2+}$	triplet	−102.378426	2.382	155.8	
U$_2$O$_2$	quintet	−253.624992	1.843; 2.450	773.6, 790.0	
U$_2$(NH)$_2$	singlet	−213.698869	1.939; 2.359	727.0, 748.0	

[a] Reference 27. [b] Reference 28. [c] Reference 29. [d] Reference 30. [e] Reference 31. [f] Reference 32. [g] Reference 33. [h] Reference 34.

Scheme 1. The Valence Molecular Orbitals Forming the Chemical Bond in U$_2^{2+}$

7s, 6dσ$_g$ (2.00)   6dπ$_u$ (4.00)   5fφ$_u$ (1.00)   5fδ$_g$ (1.00)   5fφ$_g$ (1.00)   5fδ$_u$ (1.00)
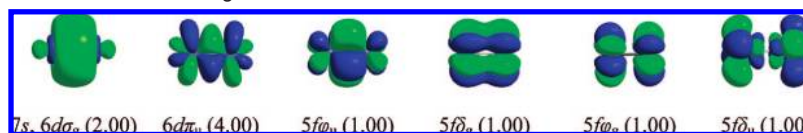
magnetic response (aromaticity/antiaromaticity), and chemical reactivity of planar isocycle and heterocycle uranium ring core structures. Here we report quantum chemical calculations on gas-phase isocyclic U$_n$X$_n$ (n = 3, 4; X = O, NH) and heterocyclic U$_n$(μ_2-X)$_n$ (n = 3, 4; X = C, NH) clusters and the E@[c-U$_4$(μ_2-C)$_4$], (E = H$^+$, C, Si, Ge) and U@[c-U$_5$(μ_2-C)$_5$] species including a planar hypervalent element E at the ring center, respectively, showing that 5f orbitals play a key role in bonding and significantly contribute to the magnetic response (diatropic/paratropic) in these f-block metal systems. In contrast to the wealth of the cluster chemistry of d-block elements, the cluster chemistry of actinides remains limited to a few examples.[6] Bare gas-phase actinide clusters have not been studied either experimentally or theoretically so far. To the best of our knowledge this is the first theoretical investigation of bare and binary gas-phase uranium clusters.

Computational Details

Extensive calculations on the optimal geometries and the ground states of the clusters were performed using scalar relativistic density functional theory (DFT) methods. The DFT route with the

BP86 functional[7,8] and a quasi-relativistic pseudopotential scheme has successfully been applied for the description of the bonding in rare earth complexes.[9] In view of the good performance of the DFT methods,[9–17] we were instigated to perform DFT calculations on all stationary points of the potential energy surfaces (PES) we studied using the Gaussian 03 program suite.[18] We performed an extensive search for the global and local minima of the clusters at the BP86/SDD(U)∪6-31G(d,p)(X) (X = nonmetal element) level of theory. In all computations no constrains were imposed on the geometry. Full geometry optimization was performed for each

(6) (a) Braun, T. P.; Simon, A.; Böttcher, F.; Ueno, F. *Angew. Chem., Int. Ed. Engl.* **1995**, *34*, 567. (b) Mokry, L. M.; Dean, N. S.; Carrano, C. J. *Angew. Chem., Int. Ed. Engl.* **1996**, *35*, 1497. (c) Duval, P. B.; Burns, C. J.; Clark, D. L.; Morris, D. E.; Scott, B. L.; Thompson, J. D.; Werkema, E. L.; Jia, L.; Andersen, R. A. *Angew. Chem., Int. Ed.* **2001**, *40*, 3357. (d) Brthet, J. C.; Thuery, P.; Ephritikhine, M. *Chem. Commun.* **2005**, 3415. (e) Ephritikhine, M. *Dalton Trans.* **2006**, 2501. (f) Gaunt, A. J.; Scott, B. L.; Neu, M. P. *Inorg. Chem.* **2006**, 7401.

(7) Perdew, J. P. *Phys. Rev. B* **1986**, *33*, 8822.
(8) Becke, A. D. *Phys. Rev. A* **1988**, *38*, 3098.
(9) (a) Wahlgren, U.; Tsushima, S.; Grenthe, I. *J. Phys. Chem. A* **2006**, *110*, 9025. (b) Wåhlin, P.; Danilo, C.; Vallet, V.; Réal, F.; Flament, J.-P.; Wahlgren, U. *J. Chem. Theory Comput.* **2008**, *4*, 569.
(10) Grimme, S.; Waletzke, M. *J. Chem. Phys.* **1999**, *111*, 5645.
(11) Wang, X.; Andrews, L. *Inorg. Chem.* **2006**, *45*, 4157.
(12) Souter, P. F.; Kushto, G. P.; Andrews, L.; Neurock, M. *J. Am. Chem. Soc.* **1997**, *119*, 1682.
(13) Cavigliasso, G.; Kaltsoyannis, N. *Inorg. Chem.* **2006**, *45*, 6828.
(14) (a) Vetere, V.; Adamo, C.; Maldivi, P. *J. Comput. Chem.* **2003**, *24*, 850. (b) Vetere, V.; Roos, B. O.; Maldivi, P.; Adamo, C. *Chem. Phys. Lett.* **2004**, *396*, 452. (c) Petit, L.; Joubert, L.; Maldivi, P.; Adamo, C. *J. Am. Chem. Soc.* **2006**, *128*, 2190.
(15) Infante, I.; Raab, J.; Lyon, J. T.; Liang, B.; Andrews, L.; Gagliardi, L. *J. Phys. Chem. A* **2007**, *111*, 11996.
(16) Michelini, M.; Russo, N.; Sicilia, E. *Angew. Chem., Int. Ed.* **2006**, *45*, 1095.
(17) (a) Lyon, J. T.; Andrews, L. *Inorg. Chem.* **2006**, *45*, 1847. (b) Lyon, J. T.; Hu, H.-S.; Andrews, L.; Li, J. *Proc. Natl. Acad. Sci. U.S.A.* **2007**, *104*, 18919. (c) Lyon, J. T.; Andrews, L.; Hu, H.-S.; Li, J. *Inorg. Chem.* **2008**, *47*, 1435.
(18) Frisch, M. J. T.; et al. *Gaussian 03*, revision B.02; Gaussian, Inc.: Pittsburgh, PA, 2003.

structure using Schlegel's analytical gradient method[19] and the attainment of the energy minimum was verified by calculating the vibrational frequencies that result in absence of imaginary eigenvalues. All stationary points have been identified for minimum (number of imaginary frequencies Nimag = 0) or transition states (Nimag = 1). The vibrational modes and the corresponding frequencies are based on a harmonic force field. This was achieved with the SCF convergence on the density matrix of at least 10^{-9} and the rms force less than 10^{-4} au. All bond lengths and bond angles were optimized to better than 0.001 Å and 0.1°, respectively. The computed electronic energies were corrected for zero-point-energy (ZPE) differences.

The natural bond orbital (NBO) population analysis was performed using Weinhold's methodology.[20,21] Wiberg bond indices (WBI), and valencies (V) were calculated using the AOMix program.[22,23] Magnetic shielding tensors have been computed with the GIAO (gauge-including atomic orbitals) DFT method[24,25] as implemented in the Gaussian 03 series of programs employing the BP86 level of theory. Nucleus-independent chemical shifts (NICS) values were computed at the BP86/SDD(U)∪6-31G(d,p)(X) level according to the procedure described by Schleyer et al.[26] The magnetic shielding tensor element was calculated for a ghost atom located at the center of the ring and along the *z*-axis. Negative (diatropic) NICS values indicate aromaticity, while positive (paratropic) values imply antiaromaticity.

Results and Discussion

Performance of the BP86/SDD(U)∪6-31G(d,p)(X) Model. We first assessed the performance of the BP86/SDD(U)∪6-31G(d,p)(X) (X = nonmetal element) model by calculating the spectroscopic parameters of some small-sized uranium species, where experimental and highly accurate theoretical data are available (Table 1).

Perusal of Table 1 reveals that the BP86/SDD(U)∪6-31G(d,p)(X) results can be compared with the experimental and the CASPT2 results, and are not found to change much. In particular the BP86/SDD(U)∪6-31G(d,p)(X) computational protocol predicts the correct ground states for all uranium species used in the benchmark calculations. Thus, the ground states for the U and U$^+$ species are predicted to be the ^5L and ^4I, respectively, the ionization energy (IE) being 5.699 eV in fairly good agreement with the experimental value.[27] The UO and UO$^+$ species adopt the ^5I and ^4I ground-state, respectively, and their calculated spectroscopic parameters are in excellent agreement with experiment (Table 1).[27] The same holds true for the US and US$^+$ species, adopting the $^5H/^5\Pi$ and $^4H/^4\Pi$

ground states, respectively. The UC diatomic adopts a $^5\Pi$ ground state, while the cation UC$^+$ prefers the $^2\Delta$ as the ground state. The U(NH) and U(NH)$^+$ species exhibit the quintet and the quartet as the ground states, respectively.

Laser-ablated U atoms reacting with CO in excess argon produce CUO, which is trapped in a triplet state in solid argon but in a linear singlet state in solid neon matrix.[30] The calculated BP86/SDD(U)∪6-31G(d,p)(X) spectroscopic parameters of CUO molecules in both the $^3\Phi$ and $^1\Sigma^+$ states are in good agreement with experiment[30] and theoretical data obtained at the more sophisticated CASPT2-s level of theory.[31] Noteworthy is the excellent agreement of the calculated spectroscopic parameters of the NUO, NUO$^+$, and NUN species with those calculated at the more sophisticated CASPT2-s level of theory.[31] The experimentally determined $\nu(\sigma_u)$ vibrational frequency of NUN in the $^1\Sigma^+$ ground state[32] is 1077 cm^{-1}.

The BP86/SDD(U) computational protocol performs also quite well in the correct description of the bonding in the ground states of binuclear uranium U$_2{}^{2+}$ species. Quantum chemical calculations at the CASPT2 level including relativistic effects showed that the U$_2{}^{2+}$ species exhibits a large number of low-lying states with *S* of 0 to 2, which share a very small bond length of about 2.30 Å.[34] The BP86/SDD(U) calculated U−U bond length of 2.130 and 2.380 Å for the singlet and triplet states, respectively, is in good accordance with the value of about 2.30 Å for the low-lying states (singlet, triplet, quintet) of U$_2{}^{2+}$ diatomic computed at the CASPT2 level.[34] Moreover, the valence molecular orbitals (Scheme 1) of U$_2{}^{2+}$ for the quintet state are similar to those computed at the CASPT2 level.

It is worthwhile to note the good performance of the BP86/SDD(U)∪6-31G(d,p)(X) computational protocol in describing the structural features of the ^1A_g ground-state of PhUUPh as compared with the CASPT2 results.[35] Thus, the BP86/SDD(U)∪6-31G(d,p)(X) and (CASPT2) computational schemes predicted the U−U bond distance equal to 2.287 (2.286 Å), the U−C bond distance equal to 2.418 (2.315 Å), and the UCU and CUC bond angles equal to 56.5 (59.2°) and 121.4 (120.8°), respectively. The computed U=O bond distances of 1.830 and 1.833 Å compare well with the U=O bond distance of 1.828 Å in the OUCO molecule,[36] and 1.838 Å determined experimentally for the diatomic UO molecule. It is also very close to the estimated U=O bond distances of 1.833−1.846 Å in the CUO(Ng) (Ng = Ar, Kr, Xe) species trapped in noble-gas matrices.[30−32]

The computed U=NH bond distances in **3** and **4** being 1.932 and 1.940 Å, respectively, compare well with the U=NPh bond distance of 2.019 Å in the (MeC$_5$H$_4$)$_3$UNPh complex determined by X-ray crystallography.[37] It is interesting to note that the Th=NH bond length in thorimine (H$_2$Th=NH) was found to

(19) Schlegel, H. B. *J. Comput. Chem.* **1982**, *3*, 214.

(20) Reed, A. E.; Curtiss, L. A.; Weinhold, F. *Chem. Rev.* **1988**, *88*, 899.

(21) Weinhold, F. *In The Encyclopedia of Computational Chemistry*; Schleyer, P. v. R., Ed.; John Wiley & Sons: Chichester, U.K., 1998; pp 1792−1811.

(22) Gorelsky, S. I. *AOMixProgram for Molecular Orbital Analysis*; York University: Toronto, Canada. http://www.sg-chem.net (accessed 1-02-2008).

(23) Gorelsky, S. I.; Lever, A. B. P. *J. Organomet. Chem.* **2001**, *635*, 187.

(24) Ditchfield, R., D. *Mol. Phys.* **1974**, *27*, 789.

(25) Gauss, J. *J. Chem. Phys.* **1993**, *99*, 3629.

(26) (a) Schleyer, P. v. R.; Maerker, C.; Dransfeld, A.; Jiao, H.; Hommes, N. J. R. v. R. *J. Am. Chem. Soc.* **1996**, *118*, 6317. (b) Chen, Z.; Wannere, C. S.; Corminboeuf, C.; Puchta, R.; Schleyer, P. v. R. *Chem. Rev.* **2005**, *105*, 3842.

(27) (a) Kaledin, L. A.; McCord, J. E.; Heaven, M. C. *J. Mol. Spectrosc.* **1994**, *164*, 27. (b) Malli, G. L. *ACS Symp. Ser.* **1989**, *394*, 291. (c) Pattoret, A.; Drowart, J.; Smoes, S. *Thermodynamics of Nuclear Materials*; IAEA: Vienna, Austria, 1968; pp 613−636.

(28) Paulovič, J.; Gagliardi, L.; Dyke, J. M.; Hirao, K. *J. Chem. Phys.* **2005**, *122*, 144317.

(29) Liang, B.; Andrews, L.; Ismail, N.; Marsden, C. *J. Inorg. Chem.* **2002**, *41*, 2811.

(30) (a) Andrews, L.; Liang, B.; Li, J.; Bursten, B. E. *New J. Chem.* **2004**, *28*, 289. (b) Liang, B.; Andrews, L.; Li, J.; Bursten, B. E. *Inorg. Chem.* **2004**, *43*, 882. (c) Andrews, L.; Liang, B.; Li, J.; Bursten, B. E. *J. Am. Chem. Soc.* **2003**, *125*, 3126. (d) Liang, B.; Andrews, L.; Li, J.; Bursten, B. E. *Chem. Eur. J.* **2003**, *9*, 4781.

(31) Gagliardi, L.; Roos, B. O.; Hirao, K. *Chem. Phys. Lett.* **2000**, *331*, 229.

(32) Clavaguéra-Sarrio, C.; Ismail, N.; Marsden, C. J.; Bégué, D.; Pouchan, C. *Chem. Phys.* **2004**, *302*, 1.

(33) Zhou, M.; Andrews, L. *J. Chem. Phys.* **1996**, *111*, 11044.

(34) (a) Gagliardi, L.; Pyykkö, P. *Angew. Chem., Int. Ed.* **2004**, *43*, 1573. (b) Gagliardi, L.; Pyykkö, P.; Roos, B. O. *Phys. Chem. Chem. Phys.* **2005**, *7*, 2415.

(35) La Macchia, G.; Brynda, M.; Gagliardi, L. *Angew. Chem., Int. Ed.* **2006**, *45*, 6210.

(36) Andrews, L.; Zhou, M.; Liang, B.; Li, J.; Bursten, B. E. *J. Am. Chem. Soc.* **2000**, *122*, 11440.

(37) Brennan, J. G.; Andenen, R. A. *J. Am. Chem. Soc.* **1985**, *107*, 514.

be 1.966 Å at the CCSD level.[38] The U=NH bond becomes shorter in the 3D tetrahedral geometry of the $U_4(NH)_4$ cluster. Moreover, in the tetrahedral geometry the U−U bond is elongated by 0.037 Å with respect to the planar stereochemistry.

In summary our theoretical results for the various uranium-containing species listed in Table 1 can be viewed as quite sound, and thereby reinforces the application of the BP86/SDD(U)∪6-31G(d,p)(X) computational protocol for the description of the structure, bonding, and magnetic response features and chemical reactivity of the isocyclic U_nX_n ($n = 3, 4$; X = O, NH) and heterocyclic $U_n(\mu_2-X)_n$ ($n = 3, 4$; X = C, NH) clusters and the E@[c-$U_4(\mu_2$-C)$_4$], (E = H, C, Si, Ge) and U@[c-$U_5(\mu_2$-C)$_5$]$^+$ species.

Equilibrium Geometries of the Isocyclic U_nX_n ($n = 3, 4$; X = O, NH) Clusters. Let us first discuss the most prominent structural features of the stationary points located on the potential energy surface (PES) of the U_nX_n ($n = 3, 4$; X = O, NH) systems. The equilibrium geometries along with selected bond lengths and angles of the U_nX_n ($n = 3, 4$; X = O, NH) clusters are shown in Figure 1.

For the U_3O_3 and $U_3(NH)_3$ systems only the planar triangular U_3 ring core structures involving one terminal oxo- or imido-ligand per uranium metal center were located as minima in the PES. All attempts to locate the $cyclo$-$U_3(\mu_2$-X)$_3$ (X = O, NH) structures were unsuccessful, owing to SCF convergence problems. The same holds also true for the U_4O_4 system; the only structure being able to locate on the PES is the four-membered U_4 ring core structure with terminal oxo-ligands. The SCF convergence problems often encountered in the quantum chemical investigation of the actinide chemistry[39] did not allow the location in the PES of the $cyclo$-$U_4(\mu_2$-O)$_4$ and the 3D tetrahedral structures. Similarly, searching the PES of higher multiplicities, we were faced with the same SCF convergence problems due to the open f-shell problem of uranium. Certainly, the correct description of the higher multiplicity structures should be given by multireference computational techniques (CASSCF/CASPT2), but calculations at those two levels are cumbersome for the size of the molecules under study.

The computed intermetallic U···U distances found in the range of 2.539−2.551 Å are indicative of strong metal−metal interactions. The U−U distances are less than those expected by the van der Waals radius for U (1.86 Å). The U−U bond distance in uranium metal is 2.77 Å, while in the diatomic U_2 molecule it was predicted to be 2.43 Å at the CASPT2/CASSI-SO level.[2]

Equilibrium Geometries of the Heterocyclic $cyclo$-U_n-$(\mu_2$-X)$_n$ ($n = 3, 4$; X = C, CH, NH) Clusters. The equilibrium geometries along with selected bond lengths and angles of the heterocyclic $cyclo$-$U_n(\mu_2$-X)$_n$ ($n = 3, 4$; X = C, CH, NH) clusters are shown in Figure 2.

It can be seen that in the $cyclo$-$U_3(\mu_2$-C)$_3$ and $cyclo$-$U_4(\mu_2$-C)$_4$ clusters exhibiting equilateral triangle and square planar ring core structures of D_{3h} and D_{4h} symmetry, respectively, the U−U bond distances of 2.923 and 3.467 Å strongly suggest the existence of U···U interactions, while in the $cyclo$-$U_4(\mu_2$-CH)$_4$

and $cyclo$-$U_4(\mu_2$-NH)$_4$ clusters such interactions seems to be negligible. The CH and NH bridges significantly enlarge the planar eight-membered metallacycle rings compared to the U_4C_4 eight-membered ring. In particular, the U−U bond distance in the $cyclo$-$U_4(\mu_2$-CH)$_4$ cluster is nearly equal to the sum of the van der Waals radii of U atoms. Both the perfect planarity and the U−X bond length equalization in the six- and eight-membered ring structures of the $cyclo$-$U_n(\mu_2$-X)$_n$ ($n = 3, 4$; X = C, CH, NH) clusters are conventionally good indicators of aromaticity in these molecules, a property which will be discussed latter on.

Stability of the Isocyclic U_nX_n ($n = 3, 4$; X = O, NH) and Heterocyclic $U_n(\mu_2$-X)$_n$ ($n = 3, 4$; X = C, CH, NH) Clusters. The stability of the $cyclo$-U_nX_n ($n = 3, 4$; X = O, NH) and $cyclo$-$U_n(\mu_2$-X)$_n$ ($n = 3, 4$; X = C, CH, NH) clusters were investigated by calculating the binding energies, ΔE_1, for their formation from the "free" U and X moieties. Moreover, we calculated the dissociation energies, ΔE_2, for the dissociation of the $cyclo$-U_nX_n ($n = 3, 4$; X = O, NH) and $cyclo$-$U_n(\mu_2$-X)$_n$ ($n = 3, 4$; X = C, CH, NH) clusters to their monomeric UX species. The calculated binding ΔE_1 and dissociation ΔE_2 energies are compiled in Table 2.

It can be seen that all $cyclo$-U_nX_n ($n = 3, 4$; X = O, NH) and $cyclo$-$U_n(\mu_2$-X)$_n$ ($n = 3, 4$; X = C, CH, NH) clusters are predicted to be bound with respect to their dissociation either to "free" U and X moieties in their ground states or to UX monomers. The calculated binding energies found to be in the range of −212.3 to −557.7 kcal/mol depend on the nature of the terminal or bridging X moiety following the trend: O > C ≈ CH > NH.

It is worth noting that for the UO diatomic molecule BP86/SDD(U)∪6-31G(d,p)(O) predicts a D_e value of 6.86 eV which is close to the D_e value of 7.43 eV computed at the CASPT2/CASSI-SO level.[34] The estimated dissociation energies for the adiabatic dissociation of the U_nX_n ($n = 3, 4$; X = O, CH, NH) clusters amounts to 40−47 kcal per mol of UX monomer, with the U_3C_3 and U_4C_4 clusters exhibiting the higher dissociation energies, which amounted to 88.8 and 101.2 kcal per mole of the UC monomer, respectively. These values are comparable to the bond dissociation energy of the U_2 diatomic molecule involving a quintuple U−U bond which was found to be 40.2 and 30.5 kcal mol^{-1} at the CASPT2 and CASPT2-SO levels,[2] respectively. For the $cyclo$-$U_4(NH)_4$ species where three possible isomers have been located on the PES the $cyclo$-$U_4(\mu_2$-NH)$_4$ isomer, **9**, corresponds to the global minimum, while the $cyclo$-$U_4(NH)_4$ (D_{4h}), **4**, and the tetrahedral $U_4(NH)_4$ (T_d), **5**, isomers are local minima at 20.3 and 25.7 kcal/mol higher in energy, respectively. The cyclic electron delocalization (aromaticity) in the planar structures **4** and **9** could account for the higher stability of the planar structures relative to the tetrahedral structure **5**. Moreover, the lower stability of the four-membered $cyclo$-$U_4(NH)_4$ ring with respect to the six-membered $cyclo$-$U_4(\mu_2$-NH)$_4$ ring could be attributed to the higher strain of the four-membered ring.

Electronic and Bonding Properties of the Isocyclic U_nX_n ($n = 3, 4$; X = O, NH) and Heterocyclic $U_n(\mu_2$-X)$_n$ ($n = 3, 4$; X = C, CH, NH) Clusters. To understand the structural integrity of the $cyclo$-U_nX_n ($n = 3, 4$; X = O, NH) and $cyclo$-$U_n(\mu_2$-X)$_n$ ($n = 3, 4$; X = C, CH, NH) clusters their valence molecular orbitals have been analyzed. Selected electronic, bonding, and spectroscopic parameters of the $cyclo$-U_nX_n ($n = 3, 4$; X = O, NH) and $cyclo$-$U_n(\mu_2$-X)$_n$ ($n = 3, 4$; X = C, CH, NH) clusters

(38) Wang, X.; Andrews, L.; Marsden, C. J. *Chem.−Eur. J.* **2007**, *13*, 5601.
(39) (a) Schreckenbach, G.; Hay, P. J.; Martin, R. L. *J. Comput. Chem.* **1999**, *20*, 70. (b) Willetts, A.; Gagliardi, L.; Ioannou, A. G.; Simperoe, A.; Skylaris, C.-K.; Spencer, S.; Handy, N. *Int. Rev. Phys. Chem.* **2000**, *19*, 327. (c) Batista, E. R.; Martin, R. L.; Hay, J. P.; Peralta, J. E.; Scuseria, G. E. *J. Chem. Phys.* **2004**, *121*, 2144. (d) Shamov, G. A.; Schreckenbach, G. *J. Phys. Chem. A* **2005**, *109*, 10961. (e) Shamov, G. A.; Schreckenbach, G.; Vo, T. N. *Chem.−Eur. J.* **2007**, *13*, 4932.

computed at the BP86/SDD(U)∪6-31G(d,p)(X) level are compiled in Table 3.

The valence of the uranium atom (atomic number 92) in the *cyclo*-U_3O_3 (D_{3h}), **1**, and *cyclo*-U_4O_4 (D_{4h}), **2**, clusters is around eight, which means that two valencies are used for the formation of a double U=O bond and the other six valencies are used to form U−U bonds with the neighboring uranium atoms in the U_3 and U_4 rings, exhibiting a partial triple bond character. This is the first example of three- and four-membered rings with partial triple bonds between all pairs of adjacent atoms involving σ-, π-, and δ-type bonds coming from the overlap of the 5f atomic orbitals (AOs) of the uranium atoms. The partial triple bond character of the U−U bond in the *cyclo*-U_3O_3 and *cyclo*-U_4O_4 clusters is reflected on the estimated Wiberg bond indices (WBI) of the U−U bonds of 2.735 and 2.478, respectively. Moreover, the oxo-ligand valency of 2.02 and 2.06 and the WBIs of the U=O bonds around 2.0 are consistent with their double bond character.

In the *cyclo*-$U_3(NH)_3$ (D_{3h}), **3**, *cyclo*-$U_4(NH)_4$ (D_{4h}), **4**, and $U_4(NH)_4$ (T_d), **5**, clusters the uranium atoms dispose of two of the valencies for the formation of a double bond with the terminal NH group, while the remaining valencies account for the formation of partial triple and double U−U bonds, respectively. The character of the U−U bonds in **3**, **4**, and **5** is reflected on the WBI(U−U) values of 2.644, 2.312, and 2.105, respectively. On the other hand, the imido-ligand valency around 3 and the WBI(U−X) values around 2.0 are consistent with the double bond character of the U−NH bonds.

In the *cyclo*-$U_3(\mu_2\text{-}C)_3$ (D_{3h}), **6**, and *cyclo*-$U_4(\mu_2\text{-}C)_4$ (D_{4h}), **7**, clusters the U and C atom's valencies indicate the formation of consecutive U−C bonds in the six- and eight-membered rings having partially double bond character. The partial double bond character of all U−C bonds is reflected on the WBI(U−C) values of 1.593 and 1.733, respectively. Noteworthy is the existence of strong U⋯U interactions in both **6** and **7**, which according to the WBI(U−U) values of 1.779 and 1.206 correspond to partially double and single U−U bonds, respectively. In contrast, in the *cyclo*-$U_4(\mu_2\text{-}CH)_4$ (D_{4h}), **8**, and *cyclo*-$U_4(\mu_2\text{-}NH)_4$ (D_{4h}), **9**, clusters the U⋯U interactions are weaker corresponding to U−U bond orders of 0.528 and 0.744, respectively. In **8** and **9** the WBI(U−X) values of 1.265 and 0.868 are indicative of U−X single bonds.

Each uranium atom in the U_3 and U_4 rings of clusters **1−5** acquires a positive natural atomic charge around 0.9−1.0 |e| gaining 1.1−1.0 |e| electron density from the coordinated oxo- and imido-ligands. In clusters **6−9** the uranium metal centers acquire a higher positive natural atomic charge amounting to 1.3−1.7 |e|. Moreover, according to the natural electron configuration of the U centers there is an increase of the occupation of the 5f orbitals of the uranium centers illustrating that these orbitals are primarily involved in direct metal−metal bonding. The bonding in *cyclo*-U_nX_n (n = 3, 4; X = O, NH) and *cyclo*-$U_n(\mu_2\text{-}X)_n$ (n = 3, 4; X = C, CH, NH) molecules is characterized by a common ring-shaped electron density, more commonly seen in aromatic organic molecules and in "all-metal" aromatics.[3–5] The 3D contour surfaces of the valence molecular orbitals describing the cyclic delocalization of the electron density in the *cyclo*-U_nX_n (n = 3, 4; X = O, NH) and *cyclo*-$U_n(\mu_2\text{-}X)_n$ (n = 3, 4; X = C, CH, NH) clusters are depicted pictorially in Figures 3 and 4, respectively.

Perusal of Figure 3 reveals that the U_3 and U_4 rings exhibit a composite bonding mode involving σ, π, δ, and φ components. Noteworthy is the presence of highly delocalized σ-, π-, δ-,

and φ-type molecular orbitals (MOs) resulting from a completely bonding interaction of the 5f AOs of each U atom. The delocalized σ, π, δ and φ electron density in the rings could be associated with the cyclic delocalization of electron density, which is a characteristic feature of multiple aromaticity. Thus, the highest ocuppied molecular orbital (HOMO) is a φ-type MO constructed from the overlap of 5f AOs (linear combination of $5f_0$ and $5f_{\pm 2}$ AOs) on each U atom. HOMO-3 of *cyclo*-U_3O_3 and *cyclo*-$U_3(NH)_3$, HOMO-4 of *cyclo*-U_4O_4, and HOMO-5 of *cyclo*-$U_4(NH)_4$ are δ-type MOs constructed from the in-phase interaction of 5f AOs (linear combination of $5f_{-3}$ and $5f_{+1}$ AOs) on each U atom. HOMO-4 of *cyclo*-U_3O_3 and *cyclo*-$U_3(NH)_3$ and HOMO-3 of *cyclo*-U_4O_4 and *cyclo*-$U_4(NH)_4$ correspond to π-type MOs that come from the overlap of 5f AOs (linear combination of $5f_0$ and $5f_{\pm 2}$ AOs) of the U metal centers. Finally, HOMO-5 of *cyclo*-U_3O_3, HOMO-6 of *cyclo*-$U_3(NH)_3$, and HOMO-7 of *cyclo*-U_4O_4 and *cyclo*-$U_4(NH)_4$ are σ-type MOs constructed from the in-phase interaction of $5f_{-3}$ AOs on each U atom. From the detailed analysis of the chemical bonding it can be concluded that the set of the totally delocalized multicenter φ, δ, π, and σ bonds constructed primarily from the overlap of 5f orbitals of the U metal centers renders f orbital aromaticity in the U_3 and U_4 "all-metal" rings. A similar valence molecular orbital pattern describing the cyclic electron density delocalization is followed by the *cyclo*-$U_n(\mu_2\text{-}X)_n$ (n = 3, 4; X = C, CH, NH) clusters (Figure 4). The most important highly delocalized MOs result from the overlap of the 5f, 7s,5f, or 7s6d5f hybridized AOs of the ring U atom. Moreover, in some of these orbitals participation of proper AOs of the bridging moieties supports the cyclic electron density delocalization in the six- and eight-membered metallacycle rings.

Magnetic Response of the Isocyclic U_nX_n (n = 3, 4; X = O, NH) and Heterocyclic $U_n(\mu_2\text{-}X)_n$ (n = 3, 4; X = C, CH, NH) Clusters. Planarity, high stability, and bond length equalization are conventionally good indicators of aromaticity, but this is restrictive in many examples. At present the nucleus-independent chemical shifts (NICS), proposed by Schleyer and co-workers,[26] is an efficient and simple criterion in probing the aromaticity/antiaromaticity of a molecule, which is based on the negative of the magnetic shielding computed, for example, at or above the geometrical centers of rings or clusters. It has been known that a negative NICS indicates that the corresponding structure is aromatic, while a positive NICS indicates that the structure is antiaromatic.

The computed NICS values at the geometrical centers of the U_3 and U_4 rings, NICS(0), and 1.0 Å above, NICS(1) are compiled in Table 4.

However, because the isotropic NICS(0) values at ring centers do not reflect the "ring current" the out-of-plane zz-components of the shielding tensor element $NICS_{zz}(0)$ and $NICS_{zz}(1)$ was proposed as a superior aromaticity measure index.[40] Applying the most fundamentally grounded magnetic criterion of aromaticity, viz. $NICS_{zz}(0)$ and $NICS_{zz}(1)$ we were able to diagnose a high diatropic response for the isocyclic U_nX_n (n = 3, 4; X = O, NH) and heterocyclic $U_n(\mu_2\text{-}X)_n$ (n = 3, 4; X = C, CH, NH) clusters.

The high negative values of the out-of-plane *zz* tensor component $NICS_{zz}(0)$ (−135 to − 353 ppm) and $NICS_{zz}(1)$ (−40

(40) (a) Schleyer, P. v. R.; Maerker, C.; Dransfeld, A.; Jiao, H.; Hommes, N. J. R. v. E. *J. Am. Chem. Soc.* **1996**, *118*, 6317. (b) Fallah-Bagher-Shaidaei, H.; Wannere, C. S.; Corminboeuf, C.; Puchta, R.; Schleyer, P. v. R. *Org. Lett.* **2006**, *8*, 863. (c) Wodrich, M. D.; Corminboeuf, C.; Park, S. S.; Schleyer, P. v. R. *Chem.—Eur. J.* **2007**, *13*, 4582.
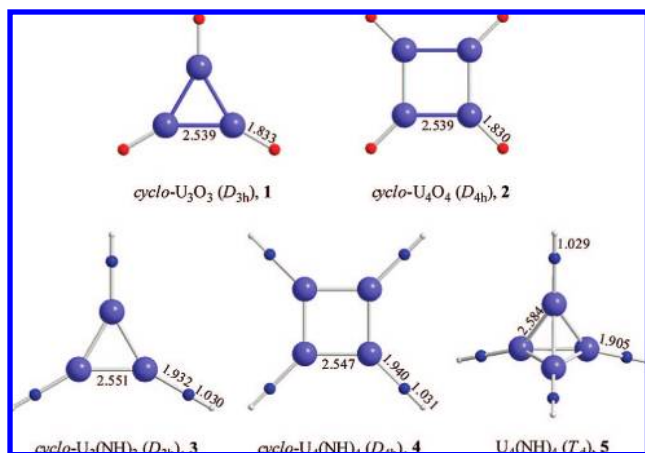
Figure 1. Equilibrium geometries (bond lengths in Å, angles in deg) of the U_nX_n ($n = 3, 4$; X = O, NH) clusters computed at the BP86/SDD(U)∪6-31G(d,p)(X) level.
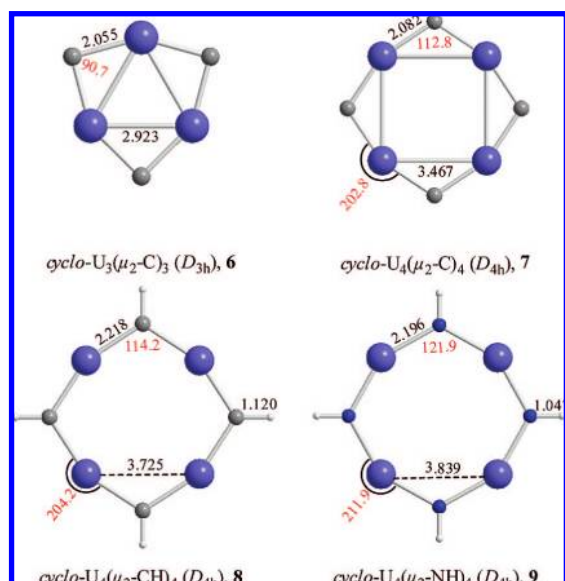

Figure 2. Equilibrium geometries (bond lengths in Å, angles in deg) of the heterocyclic *cyclo*-$U_n(\mu_2$-X$)_n$ ($n = 3, 4$; X = C, CH, NH) clusters computed at the BP86/SDD(U)∪6-31G(d,p)(X) level.

to -171 ppm), are indicative for the high aromatic character of the *cyclo*-U_nX_n ($n = 3, 4$; X = O, NH) and *cyclo*-$U_n(\mu_2$-X$)_n$ ($n = 3, 4$; X = C, CH, NH) clusters. To the best of our knowledge there is no precedent for such huge NICS values reported so far. It is interesting to compare the high NICS$_{zz}$(1) values of the uranium metallacycles with the much lower NICS$_{zz}$(1) values of the related ruthenium metallacycles reported previously.[41] Compare also the NICS values of the aromatic three-member U_3 ring with those of the three-membered Mg_3^{n-} ($n = 0, 1, 2$) ring exhibiting very low aromaticity.[42] The NICS(0) values, except for the *cyclo*-$U_3(\mu_2$-C$)_3$, **6**, cluster are positive (2 to 136 ppm), with the *cyclo*-$U_3(NH)_3$ (D_{3h}), **3**, cluster having the higher value (136.0 ppm), which is indicative of paratropicity (anti-aromaticity). This could be due to the paratropic contribution of the in-plane shielding tensor component to the NICS(0)

Table 2. Total Electronic E_{tot}, Binding ΔE_1, and Dissociation Energies ΔE_2 (in kcal/mol) of the Dissociation of the *cyclo*-U_nX_n ($n = 3, 4$; X = O, NH) and *cyclo*-$U_n(\mu_2$-X$)_n$ ($n = 3, 4$; X = C, CH, NH) Clusters to Their Monomeric UX species Computed at the BP86/SDD(U)∪6-31G(d,p)(X) Level

cluster	E_{tot}	$\Delta E_1{}^a$	$\Delta E_2{}^b$	ΔE_2/mol UX
cyclo-U_3O_3 (D_{3h}), **1**	-380.403265	-403.1	119.9	40.0
cyclo-U_4O_4 (D_{4h}), **2**	-507.236681	-557.7	180.2	45.0
cyclo-$U_3(NH)_3$ (D_{3h}), **3**	-320.573698	-212.3	106.9	35.6
cyclo-$U_4(NH)_4$ (D_{4h}), **4**	-427.471351	-308.0	167.6	41.9
$U_4(NH)_4$ (T_d), **5**	-427.462697	-302.6	162.1	40.5
cyclo-$U_3(\mu_2$-C$)_3$ (D_{3h}), **6**	-268.565547	-285.6	266.4	88.8
cyclo-$U_4(\mu_2$-C$)_4$ (D_{4h}), **7**	-358.166164	-430.2	404.7	101.2
cyclo-$U_4(\mu_2$-CH$)_4$ (D_{4h}), **8**	-360.581761	-430.0	24.1	6.0
cyclo-$U_4(\mu_2$-NH$)_4$ (D_{4h}), **9**	-427.503715	-328.3	187.8	47.0

^{a} $\Delta E_1 = E(cyclo$-$U_nX_n) - [nE(U) + nE(X)]$. ^{b} $\Delta E_2 = nE(UX) - E(cyclo$-$U_nX_n)$.

values. On the other hand, the NICS(1) values, except for clusters **1**, **3**, and **9** are negative (-4.9 to -39.2 ppm) associated with a diatropic response.

To get a better insight into the origin of the aromaticity of the *cyclo*-U_nX_n ($n = 3,4$; X = O, NH) and *cyclo*-$U_n(\mu_2$-X$)_n$ ($n = 3, 4$; X = C, CH, NH) clusters we also applied the NICS scan procedure which is based on scanning the NICS, σ(bq), values over a distance R and dissecting them into in-plane, σ(bq$_{in}$) and out-of-plane, σ_{zz}(bq$_{out}$) components.[42,43] Illustrative NICS scan pictures for representative uranium clusters are given in Figure 5.

The picture obtained from the NICS-scan procedure is indicative of diamagnetic and paramagnetic ring currents and thus can be rationalized in a much more consistent way than a single NICS value.[43] It can be seen that the NICS scans show clearly that all the clusters under study have different magnitudes of diatropic ring currents, and thus all of them are aromatic molecules.

Equilibrium Geometries Stability and Bonding Properties of the E@[*cyclo*-$U_4(\mu_2$-C$)_4$], (E = H$^+$, C, Si, Ge) and U@[*cyclo*-$U_5(\mu_2$-C$)_5$] Clusters. Let us first discuss the most prominent structural features of the E@[*cyclo*-$U_4(\mu_2$-C$)_4$], (E = H$^+$, C, Si, Ge) and U@[*cyclo*-$U_5(\mu_2$-C$)_5$] clusters. Selected bond lengths and angles of the E@[*cyclo*-$U_4(\mu_2$-C$)_4$], (E = H$^+$, C, Si, Ge) and U@[*cyclo*-$U_5(\mu_2$-C$)_5$] molecules computed at the BP86/SDD(U)∪6-31+G(d,p)(E) level are shown in Figure 6.

The most striking structural feature of the H@[*cyclo*-$U_4(\mu_2$-C$)_4$]$^+$ and H@[*cyclo*-$U_4(\mu_2$-CH$)_4$]$^+$ molecules is the planar four-coordinated hydrogen atom captured at the center of the U_4 ring core structure, which is coordinated with the four ring uranium atoms. The calculated U–H bond distances in **10** and **14** were found equal to 2.509 and 2.628 Å, respectively. This is the first example of planar tetracoordinate hydrogen (ptH) stabilized by four-membered ring perimeters composed of four uranium atoms. Very recently,[44] a tetracoordinate hydrogen atom coordinated to four Y atoms in a tetrahedral coordination environment has been unambiguously located, by single-crystal neutron diffraction for the first time, in the center of the tetrahedral metal complex $Y_4H_8(Cp')_4(THF)[Cp']C_5Me_4$-(SiMe$_3$)]. Moreover, tetracoordinate protons have recently been identified in a new type

(41) Tsipis, A. C.; Kefalidis, C. E.; Tsipis, C. A. *J. Am. Chem. Soc.* **2007**, *129*, 13905.

(42) (a) Poater, J.; Bofill, J. M.; Alemany, P.; Solà, M. *J. Org. Chem.* **2006**, *71*, 1700. (b) Jiménez-Halla, J. O. C.; Matito, E.; Robles, J.; Solà, M. *J. Organomet. Chem.* **2006**, *691*, 4359.

(43) (a) Stanger, A. *J. Org. Chem.* **2006**, *71*, 883. (b) Stanger, A. *Chem.—Eur. J.* **2006**, *12*, 2745.

(44) Yousufuddin, M.; Gutmann, M. J.; Baldamus, J.; Tardif, O.; Hou, Z.; Mason, S. A.; McIntyre, G. J.; Bau, R. *J. Am. Chem. Soc.* **2008**, *130*, 3888.

Table 3. Selected Electronic, Bonding, and Spectroscopic Parameters of the *cyclo*-U_nX_n (n = 3, 4; X = O, NH) and *cyclo*-$U_n(\mu_2\text{-X})_n$ (n = 3, 4; X = C, CH, NH) Clusters Computed at the BP86/SDD(U)∪6-31G(d,p)(X) Level

cluster	WBI(U–U)[a]	WBI(U–X)	V(U)[b]	V(X)	nec(U)[c] 7s/5f/6d	Q(U)[d]
cyclo-U_3O_3 (D_{3h}), **1**	2.735	2.028	7.765	2.303	0.55/4.11/0.50	0.977
cyclo-U_4O_4 (D_{4h}), **2**	2.478	2.059	8.103	2.291	0.46/4.10/0.62	0.955
cyclo-$U_3(NH)_3$ (D_{3h}), **3**	2.644	2.025	7.530	3.020	0.55/4.07/0.51	1.003
cyclo-$U_4(NH)_4$ (D_{4h}), **4**	2.312	2.023	7.787	2.990	0.44/4.07/0.64	0.971
$U_4(NH)_4$ (T), **5**	2.105	1.891	8.554	3.019	0.49/4.20/0.58	0.896
cyclo-$U_3(\mu_2\text{-C})_3$ (D_{3h}), **6**	1.779	1.593	6.895	3.461	0.64/3.71/0.53	1.276
cyclo-$U_4(\mu_2\text{-C})_4$ (D_{4h}), **7**	1.206	1.733	6.495	3.644	0.46/3.55/0.40	1.700
cyclo-$U_4(\mu_2\text{-CH})_4$ (D_{4h}), **8**	0.528	1.265	4.180	3.384	0.49/3.63/0.27	1.677
cyclo-$U_4(\mu_2\text{-NH})_4$ (D_{4h}), **9**	0.744	0.868	3.606	2.460	0.98/3.43/0.23	1.369

[a] Wiberg bond index (WBI). [b] Valences (V). [c] Natural electron configuration of uranium, nec(U). [d] Natural atomic charges.
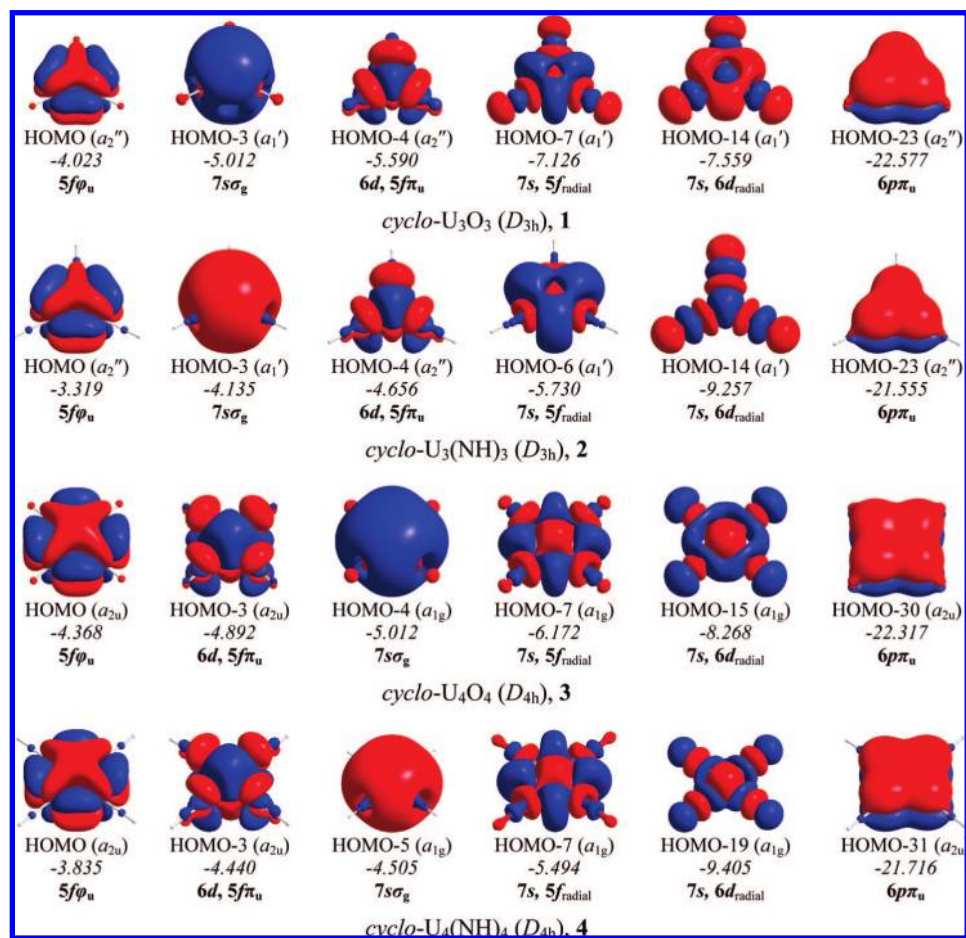
Figure 3. 3D contour surfaces of the valence molecular orbitals responsible for the cyclic delocalization of the electron density in the U_3 and U_4 rings of the *cyclo*-U_nX_n (n = 3, 4; X = O, NH) clusters (figures in italics are the orbital energies, in eV).

of exotic nonclassical carbocations forming the so-called proton sandwiches.[45] The size of the U_4 ring in the *cyclo*-$U_4(\mu_2\text{-C})_4$ cluster can also accommodate a planar tetracoordinate C (ptC) and/or Si (ptSi) atom comfortably, but it is too small to accommodate the heavier Ge atom. The latter adopts a pyramidal stereochemistry of C_{4v} symmetry with the Ge atom 1.125 Å above the ring centroid. The ptC and ptSi atoms in **11** and **12** adopt a perfect planar stereochemistry, the calculated C–U and Si–U bond lengths were found to be 2.377 and 2.659 Å, respectively. The relatively short computed M–E bond lengths indicate significant stabilization because these bond distances are shorter than the sum of van der Waals radii, for example,

for U–H (3.06 Å), U–C (3.56 Å), and U–Si (3.196 Å).[46] Attempts to design molecules containing a planar tetracoordinate carbon atom have been pursued for nearly 40 years since the initial seminal work on the subject by Hoffmann and co-workers.[47] In a landmark 1976 paper, Schleyer, Pople and co-workers took up the challenge of creating planar tetracoordinate carbon using the electronic approach.[48] The more recent results in the wider area of planarizing distortions of tetracoordinate

(45) Gutta, P.; Tantillo, D. *Angew. Chem., Int. Ed.* **2005**, *44*, 2719.

(46) Lide, D. R.; Frederikse, H. P. R. *CRC Handbook of Chemistry Physics*; CRC Press: New York, 1998; pp 9−51.
(47) Hoffmann, R.; Alder, R. W.; Wilcox, C. F., Jr. *J. Am. Chem. Soc.* **1970**, *92*, 4992.
(48) Collins, J. B.; Dill, J. D.; Jemmis, E. D.; Apeloig, Y.; Schleyer, P. v. R.; Seeger, R.; Pople, J. *J. Am. Chem. Soc.* **1976**, *98*, 5419.
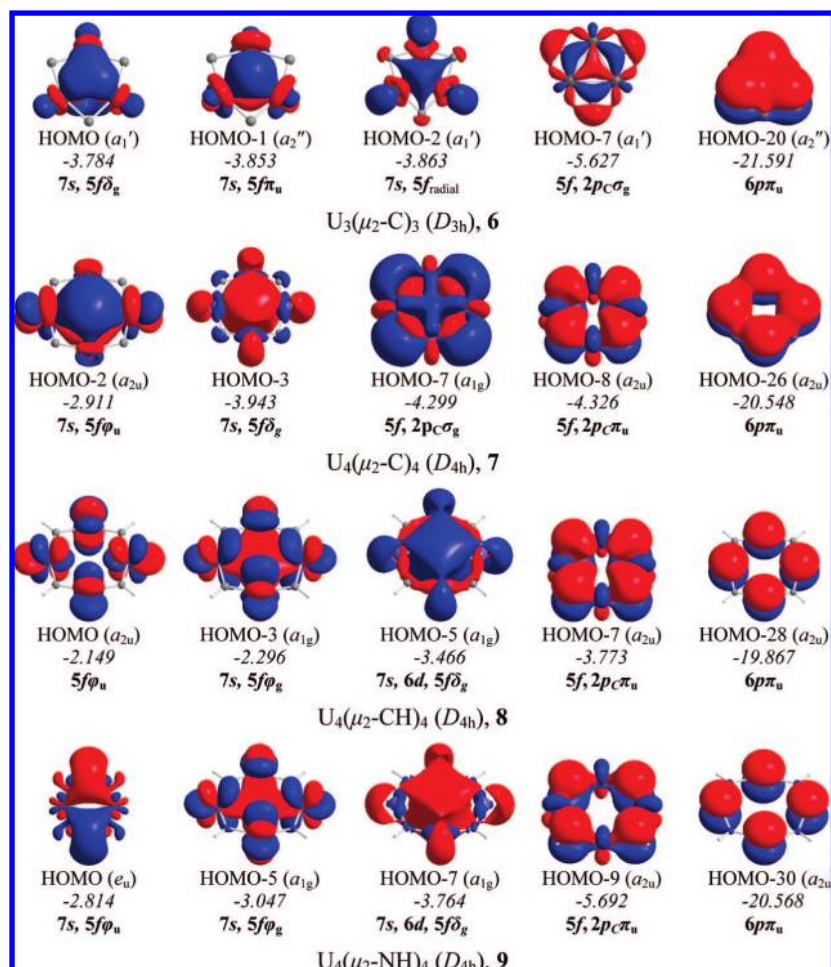
Figure 4. 3D contour surfaces of the valence molecular orbitals responsible for the cyclic delocalization of the electron density in the *cyclo*-U$_n$(μ_2-X)$_n$ (*n* = 3, 4; X = C, CH, NH) clusters (figures in italics are the orbital energies, in eV).

carbon have recently presented in *Chem. Rev.*[49] Recently, DFT calculations indicated that planar tetracoordinate carbons (ptC's) can be stabilized by four-membered ring perimeters composed of four bare transition metal atoms. Recent advances in planar tetracoordinate carbon chemistry have also been reported.[50] Moreover, sets of boron rings enclosing planar hypercoordinate group 14 elements (AB$_n^{(n-8)}$; A = group 14 element; *n* = 6−10) were designed systematically based on geometrical and electronic fit principles: the size of a boron ring must accommodate the central atom comfortably.[51]

Remarkably, the size of the five-membered U$_5$ ring in the perfectly planar U@[*cyclo*-U$_5$(μ_2-C)$_5$], **15**, cluster allowed the accommodation of a planar five-coordinated uranium atom. The calculated U−U bond lengths of the radial U−U bonds between the central and the peripheral uranium atoms (2.812 Å) are shorter than the U−U bond lengths of the U$_5$ ring.

The stability of the E@[*cyclo*-U$_4$(μ_2-C)$_4$], (E = H$^+$, C, Si, Ge) molecules are investigated using the following fragmentation scheme:

$$E@[cyclo\text{-}U_4(\mu_2\text{-}C)_4] \rightarrow cyclo\text{-}U_4(\mu_2\text{-}C)_4 + E$$
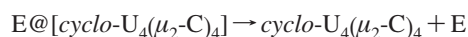
(49) Keese, R. *Chem. Rev.* **2006**, *106*, 4787.
(50) Merino, G.; Méndez-Rojas, M. A.; Vela, A.; Heine, T. *J. Comput. Chem.* **2007**, *28*, 362.
(51) Islas, R.; Heine, T.; Ito, K.; Schleyer, P. v. R.; Merino, G. *J. Am. Chem. Soc.* **2007**, *129*, 14767.

Table 4. The NICS Values[a]

cluster	NICS(0)	NICS(1)	NICS$_{zz}$(0)	NICS$_{zz}$(1)
cyclo-U$_3$O$_3$ (*D$_{3h}$*), **1**	128.9	32.2	−342.3	−105.7
cyclo-U$_4$O$_4$ (*D$_{4h}$*), **2**	2.1	−16.9	−349.2	−170.6
cyclo-U$_3$(NH)$_3$ (*D$_{3h}$*), **3**	136.0	32.7	−337.4	−109.1
cyclo-U$_4$(NH)$_4$ (*D$_{4h}$*), **4**	6.5	−13.4	−352.5	−163.7
cyclo-U$_3$(μ_2-C)$_3$ (*D$_{3h}$*), **6**	−43.3	−39.2	−267.0	−40.1
cyclo-U$_4$(μ_2-C)$_4$ (*D$_{4h}$*), **7**	3.3	−4.6	−158.7	−76.3
cyclo-U$_4$(μ_2-NH)$_4$ (*D$_{4\ h}$*), **9**	5.9	5.1	−135.2	−65.1

[a] Given in ppm and calculated at the ring center, NICS(0) and 1.0 Å above the ring center, NICS(1) along with the *zz*-component of the shielding tensor element, NICS$_{zz}$(0) and NICS$_{zz}$(1) for the *cyclo*-U$_n$X$_n$ (*n* = 3, 4; X = O, NH) and *cyclo*-U$_n$(μ_2-X)$_n$ (*n* = 3, 4; X = C, NH) clusters computed at the BP86/SDD(U)∪6-31G(d,p)(X) level.

The calculated dissociation energies (*DE*s) are compiled in Table 5.

According to the estimated DEs the ptH, ptC, and ptSi atoms are strongly bonded to the U$_4$ rings of the *cyclo*-[U$_4$(μ_2-C)$_4$] cluster following the trend: ptH > ptC > ptSi. The face-capping μ_4-Ge atom is bonded more weakly to the eight-membered U$_4$(μ_2-C)$_4$ ring, having a DE value of 50.5 kcal/mol. We encountered problems in the calculation of DE of the U@[*cyclo*-U$_5$(μ_2-C)$_5$] **15** cluster, for all our attempts to locate the bigger ten-membered U$_5$(μ_2-C)$_5$ ring as a minimum in the PES were unsuccessful due to SCF convergence problems.

The calculated WBI(U−E)s show the U−E bond order ranging from 0.312 to 1.317 indicates significant U−E bonding
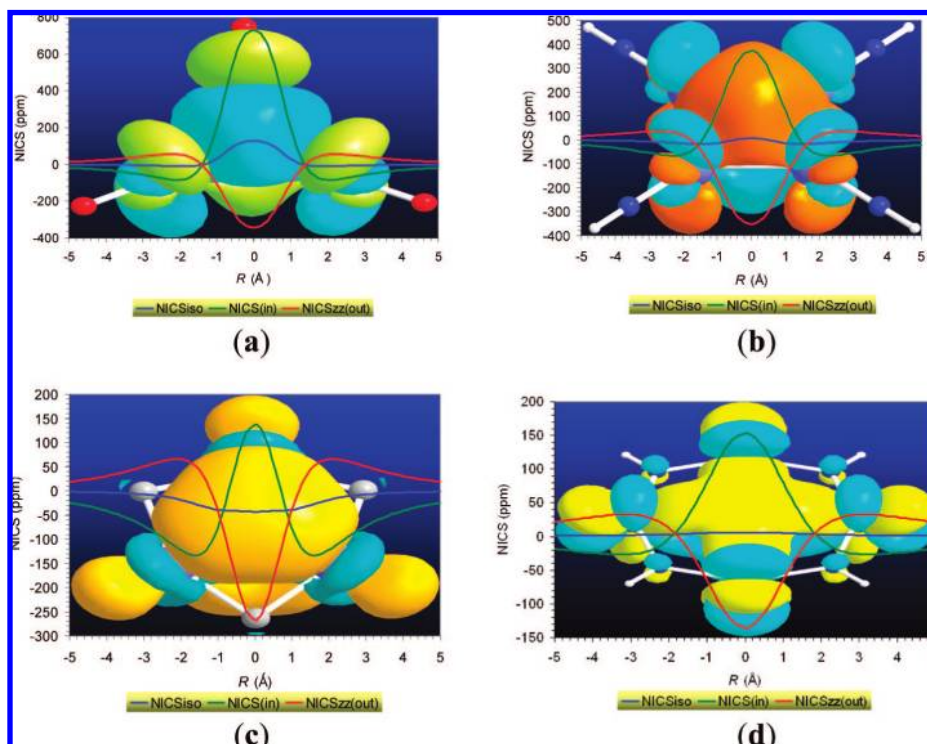
Figure 5. Illustrative NICS scan pictures for the isotropic out-of-plane, $\sigma^{iso}(bq_{out})$, the in-plane, $\sigma(bq_{in})$, and the out-of-plane, $\sigma^{zz}(bq_{out})$, tensors of the *cyclo*-U_3O_3 (D_{3h}) **1** (a), *cyclo*-$U_4(NH)_4$ (D_{4h}) **4** (b), *cyclo*-$U_3(\mu_2$-C$)_3$ (D_{3h}) **6** (c), and *cyclo*-$U_4(\mu_2$-NH$)_4$ (D_{4h}) **9** (d) molecules.
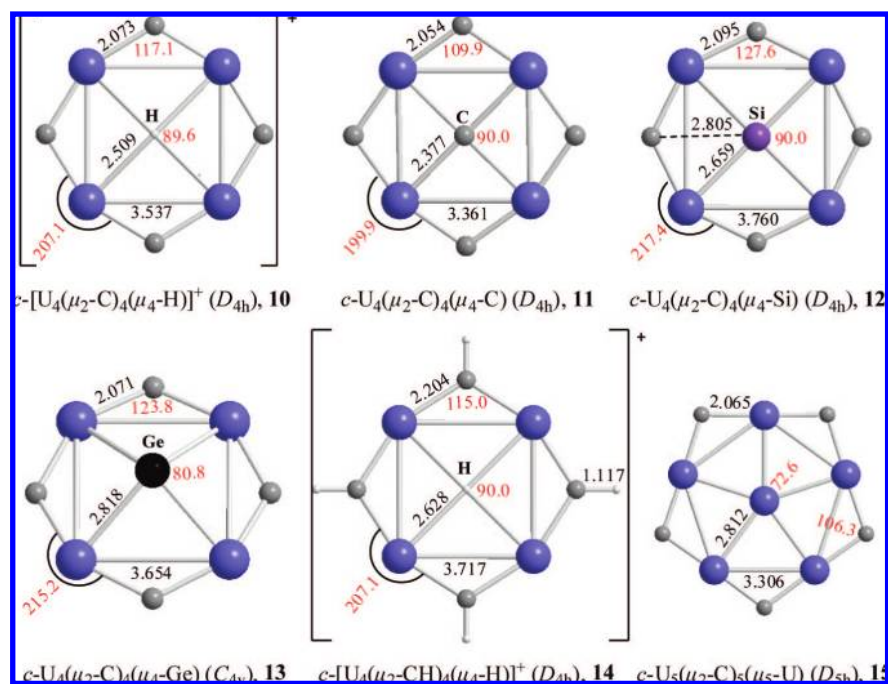

Figure 6. Equilibrium geometries (bond lengths in Å, angles in deg) of the E@[*cyclo*-$U_4(\mu_2$-C$)_4$], (E = H$^+$, C, Si, Ge) and U@[*cyclo*-$U_5(\mu_2$-C$)_5$] molecules computed at the BP86/SDD(U)$\cup$6-31+G(d,p)(E) level.

interactions. The total WBI of the central H atom ranges from 1.536 to 1.248 in **10** and **14**, respectively, indicating that each U−H bond is weak, but the number of U−H binding compensates for the weak U−H bonding interactions. However, the total WBI of the central E (E = C, Si Ge) atoms ranges as 3.700, 3.948, and 3.712 for C, Si, and Ge, respectively, indicating that each U−E bond corresponds nearly to a single U−E bond. The same holds true for cluster **15** where the total

WBI of 5.508 of the central U atom indicates the formation of five single U−U bonds with the five ring uranium atoms.

Molecular orbital analyses of **10**−**15** reveals features that stabilize the planar H$^+$, C, and Si atoms accommodated in the center of the four-member U_4 ring in **10**, **11**, **12**, and **14**, the face-capping coordination of the Ge atom to the four-member U_4 ring in **13** and the planar five-coordinate U atom accommodated in the center of the U_5 pentagon in **15**. Illustrative

Table 5. Bond Dissociation Energies, BDEs (in kcal/mol) and Selected Electronic and Bonding Parameters of the E@[*cyclo*-U$_4$(μ_2-C)$_4$], (E = H$^+$, C, Si, Ge) and U@[*cyclo*-U$_5$(μ_2-C)$_5$] Clusters Computed at the BP86/SDD(U)∪6-31+G(d,p)(E) Level

cluster	DE	WBI(U−E)	WBI(U−U)	Q(E)	Q(U)	nec(E) ns/np	nec(U) 7s/5f/6d
H@[*cyclo*-U$_4$(μ_2-C)$_4$]$^+$, **10**	269.9	0.384		−0.648	2.070	1.65	0.11/3.61/0.35
C@[*cyclo*-U$_4$(μ_2-C)$_4$], **11**	190.9	0.925	0.805	−2.100	2.051	1.75/4.32	0.21/3.54/0.38
Si@[*cyclo*-U$_4$(μ_2-C)$_4$], **12**	99.7	0.987	0.866	−0.838	1.801	1.59/3.23	0.29/3.66/0.39
Ge@[*cyclo*-U$_4$(μ_2-C)$_4$], **13**	50.5	0.928	0.895	−1.100	1.884	1.75/3.32	0.32/3.53/0.42
H@[*cyclo*-U$_4$(μ_2-CH)$_4$]$^+$, **14**	279.2	0.312	0.465	−0.716	2.030	1.71	0.14/3.67/0.24
U@[*cyclo*-U$_5$(μ_2-C)$_5$], **15**		1.377	0.926	−0.634	1.605	1.16/4.38/0.87	0.25/3.96/0.37

valence MOs of clusters **10**, **12**, and **15** are shown in Figure 7. (The full set of MOs is given in the Supporting Information).

Thus the HOMO-2, HOMO-11, and HOMO-19 of the H@[*cyclo*-U$_4$(μ_2-C)$_4$]$^+$, **10**, cluster correspond to σ-type MOs constructed from the overlap of the 1s AO of the central hydrogen atom with radial MOs delocalized over the ring U and C atoms. In all these radial MOs the U atoms dispose sdf hybridized AOs of various compositions. Natural bond orbital (NBO) analyses indicate considerable electron transfer from the surrounding uranium atoms to the more electronegative hydrogen atom, which acquires a negative natural atomic charge of −0.648 |e| in **10** and −0.716 |e| in **14**. As a consequence the natural electron configuration of the ptH's are 1.65 and 1.71 in **10** and **14**, respectively.

The bonding in the ptE's (E = C, Si, Ge) is described by three types of MOs. The first type corresponds to σ-type MOs that come from the overlap of the np$_x$ and np$_y$ AOs of the ptE's with degenerate radial MOs delocalized over the uranium ring atoms (HOMO-13,14, in **11**, HOMO-14,15 in **12**, and HOMO-12,13 in **13**). The second type corresponds also to σ-type MOs that come from the overlap of the np$_x$ and np$_y$ AOs of the ptE's with degenerate radial MOs delocalized over the uranium and carbon ring atoms (HOMO-3,4 in **11**, and HOMO-2,3 in **12** and **13**). The third type corresponds to π-type MOs constructed from the in-phase interaction of the np$_z$ AOs of the ptE's with π-type MOs delocalized over the uranium and/or the uranium and carbon ring atoms (HOMO-5 and HOMO-12 in **11**, and HOMO-4 and HOMO-11 in **12** and HOMO-4 and HOMO-9 in **13**). The molecular orbital pictures given in Figure 7 are in line with the molecular orbital picture of planar CH$_4$ proposed by Hoffmann and co-workers in 1970.[47]

NBO analyses reveals significant electron transfer from the surrounding uranium atoms to the central ptE's, which acquire negative natural atomic charges of −2.100 |e| in **11**, −0.838 |e| in **12**, and −1.100 |e| in **13**. Noteworthy are the significant np$_z$ ptE's orbital occupancies. Thus, the natural electron configuration of the central E atom is 2s$^{1.75}$2p$_x^{1.38}$2p$_y^{1.38}$2p$_z^{1.55}$ in **11**, 3s$^{1.59}$3p$_x^{1.05}$3p$_y^{1.05}$3p$_z^{1.13}$ in **12**, 4s$^{1.75}$4p$_x^{1.16}$4p$_y^{1.16}$4p$_z^{1.01}$ in **13**. The np$_z$ orbital occupancies are in line with the bonding model suggested by Wang and Schleyer,[52] which is based conceptually on stabilization of a vacant 2p$_z$ ptC AO through electron transfer.

Finally, the bonding of the planar pentacoordinate uranium atom in **15** is described by the MOs shown in Figure 7, which come from the overlap of the 5f AOs of the central U atom with radial MOs delocalized over the uranium ring atoms. The degenerate HOMO and HOMO-1 of e_2'' symmetry are π-type MOs constructed from the out-of-plane overlap of the 5f AOs of the central U atom with 5f AOs of the five peripheral U atoms. The degenerate HOMO-2 and HOMO-3 of e_2' symmetry are also π-type MOs that come from the in-plane overlap of the 5f AOs of the central U atom with 5f AOs of the five

Table 6. The NICS Values (in ppm) for the E@[*cyclo*-U$_4$(μ_2-C)$_4$], (E = H$^+$, C, Si, Ge) Clusters Computed at the GIAO/BP86/SDD(U)∪6-31G(d,p)(X) Level

cluster	NICS(0.1)	NICS(1)	NICS$_{zz}$(0.1)	NICS$_{zz}$(1)
H@[*cyclo*-U$_4$(μ_2-C)$_4$]$^+$, **10**	−9.6	−4.2	−74.5	−75.8
C@[*cyclo*-U$_4$(μ_2-C)$_4$], **11**	370.0	1.7	317.4	−23.2
Si@[*cyclo*-U$_4$(μ_2-C)$_4$], **12**	74.9	2.2	336.1	−37.9
Ge@[*cyclo*-U$_4$(μ_2-C)$_4$], **13**	−1.0	1.5	−147.3	−74.4
H@[*cyclo*-U$_4$(μ_2-CH)$_4$]$^+$, **14**	−18.6	0.06	−188.0	−90.1

peripheral U atoms. The HOMO-4 with a_2'' symmetry is a radial bonding MO that comes from the overlap of the 5f$_{z^3}$ AO of the central U atom with 5f AOs (linear combination of 5f$_0$ and 5f$_{\pm2}$ AOs) of the peripheral U atoms) each 5f AO contributing 9.81% while the contribution of the 5f$_{z^3}$ AO of the central U atom amounts to 50.5%. The degenerate HOMO-5 and HOMO-6 of e_1'' symmetry are π-type MOs constructed from the out-of-plane overlap of the 6d AOs (6d$_{\pm1}$ AOs) of the central U atom with 5f AOs of the five peripheral U atoms. According to the NBO analyses the central uranium atom acquires negative natural atomic charge of −0.716 |e|. Obviously, there is a significant charge transfer from the peripheral U atoms to the central U atom which exhibits the natural electron configuration 7s$^{1.16}$5f$_{z^3}^{1.01}$5f$_{xz^2}^{0.84}$5f$_{yz^2}^{0.83}$5f$_{xyz}^{0.82}$5f$_{z(x^2-y^2)}^{0.82}$. Note the important contribution of the perpendicular ppU 5f$_{z^3}$ orbital to the delocalized 5fπ MO of the *cyclo*-U$_5$(μ_2-C)$_5$ cluster.

Magnetic Properties of the E@[*cyclo*-U$_4$(μ_2-C)$_4$], (E = H$^+$, C, Si, Ge) and U@[*cyclo*-U$_5$(μ_2-C)$_5$] Clusters. We have also explored the electron delocalization and magnetic response of the E@[*cyclo*-U$_4$(μ_2-C)$_4$], (E = H$^+$, C, Si, Ge) and U@[*cyclo*-U$_5$(μ_2-C)$_5$] clusters. The computed NICS values of the E@[*cyclo*-U$_4$(μ_2-C)$_4$], (E = H$^+$, C, Si, Ge) clusters are compiled in Table 6.

It can be seen that the NICS$_{zz}$(1) values illustrate a diatropic magnetic response of the E@[*cyclo*-U$_4$(μ_2-C)$_4$], (E = H$^+$, C, Si, Ge) clusters associated with an appreciable cyclic electron delocalization around the metallacycle ring. For the C@[*cyclo*-U$_4$(μ_2-C)$_4$] **11** and U@[*cyclo*-U$_5$(μ_2-C)$_5$] **15** clusters we also calculated the NICS(*R*) values in some points of the periphery of a cycle with its center coincident with the metallacycle ring center and having a radius of 1.555 and 2.016 Å, respectively. Figure 8 displays the positions of the bq points on the periphery of the cycles which were placed at the molecular plane and at 1.0 and 2.0 Å above the molecular plane.

Noteworthy is the diatropic response of the C@[*cyclo*-U$_4$(μ_2-C)$_4$] and U@[*cyclo*-U$_5$(μ_2-C)$_5$] clusters reflected on the NICS$_{zz}$(0) and NICS$_{zz}$(1) values. Moreover, the estimated out-of-plane σ_{zz} carbon shielding tensor element of −281.1 ppm is consistent with the decrease of electron density at the ptC and the cyclic electron delocalization. In summary, the magnetic properties of the E@[*cyclo*-U$_4$(μ_2-C)$_4$], (E = H$^+$, C, Si, Ge) and U@[*cyclo*-U$_5$(μ_2-C)$_5$] clusters reveal that cyclic electron

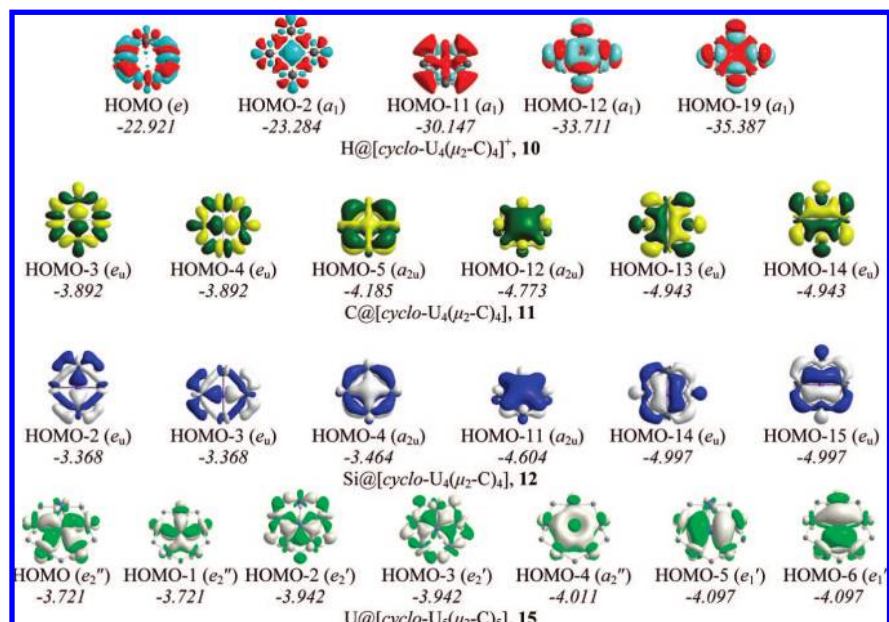(52) Wang, Z.-X.; Schleyer, P. V. R. *J. Am. Chem. Soc.* **2001**, *123*, 994.

Figure 7. 3D contour surfaces of illustrative valence molecular orbitals responsible for stabilization of the central atom in the E@[*cyclo*-U$_4$(μ_2-C)$_4$], (E = H$^+$, C, Si) and U@[*cyclo*-U$_5$(μ_2-C)$_5$] clusters (figures in italics are the orbital energies, in eV).
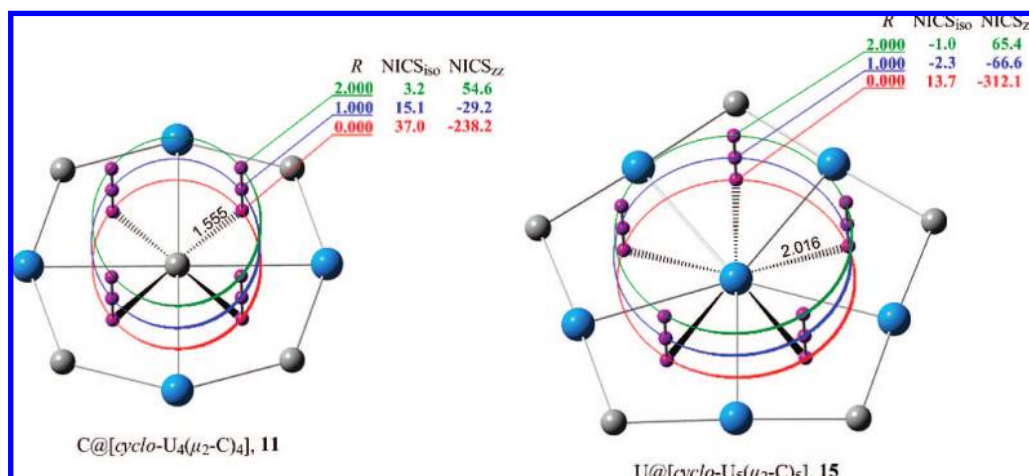
Figure 8. The bq points on the periphery of the cycles designed in the C@[*cyclo*-U$_4$(μ_2-C)$_4$] and U@[*cyclo*-U$_5$(μ_2-C)$_5$] clusters along with the respective NICS values (*R* is given in Å, and NICS values in ppm).

delocalization is a key factor for the stabilization of the ptE's inside the six- and eight-membered uranacycle rings.

Conclusions

In this paper we have demonstrated, using electronic structure calculation methods (DFT), that the model planar isocyclic *cyclo*-U$_n$X$_n$ (n = 3, 4; X = O, NH) and heterocyclic *cyclo*-U$_n$(μ_2-X)$_n$ (n = 3, 4; X = C, CH, NH) clusters are thermodynamically stable molecules with respect to their dissociation either to "free" U and X moieties or to their monomeric UX species. The size of the U$_4$ ring in the *cyclo*-U$_4$(μ_2-C)$_4$ cluster can accommodate inside the ring center a planar tetracoordinate element E (E = H, C, Si) comfortably (ptE), but it is too small to accommodate the heavier Ge atom affording thermodynamically stable E@[*c*-U$_4$(μ_2-C)$_4$], (E = H$^+$, C, Si, Ge) molecules. The larger size of the ten-membered *cyclo*-U$_5$(μ_2-C)$_5$ can capture at the center the bigger U atom in a pentacoordinate environment affording the thermodynamically stable U@[*c*-U$_5$(μ_2-C)$_5$] cluster.

All *cyclo*-U$_n$X$_n$ (n = 3, 4; X = O, NH) and *cyclo*-U$_n$(μ_2-X)$_n$ (n = 3, 4; X = C, CH, NH) clusters are predicted to be bound with respect to their dissociation to "free" U and [X] moieties in their ground states.

The estimated dissociation energies (DEs) of the E@[*c*-U$_4$(μ_2-C)$_4$], (E = H$^+$, C, Si, Ge) and U@[*c*-U$_5$(μ_2-C)$_5$] clusters indicate that the ptH, ptC, and ptSi atoms are strongly bonded to the U$_4$ rings of the *cyclo*-[U$_4$(μ_2-C)$_4$] cluster following the trend: ptH > ptC > ptSi, while the face-capping μ_4-Ge atom is bonded more weakly to the eight-membered U$_4$(μ_2-C)$_4$ ring.

The bonding in the *cyclo*-U$_n$X$_n$ (n = 3, 4; X = O, NH) and *cyclo*-U$_n$(μ_2-X)$_n$ (n = 3, 4; X = C, CH, NH) clusters is characterized by a common ring-shaped electron density, more commonly seen in aromatic organic molecules and in "all-metal" aromatics. The U$_3$ and U$_4$ ring structural cores exhibit a composite bonding mode involving σ, π, δ, and φ components. Noteworthy is the presence of highly delocalized σ-, π-, δ-, and φ-type MOs resulting from a completely bonding interaction

of the 5f AOs of each U atom of the metallacycle ring. The delocalized σ, π, δ, and φ electron density in the rings could be associated with the cyclic electron delocalization, which is a characteristic feature of multiple aromaticity.

The aromaticity of the *cyclo*-U_nX_n (n = 3, 4; X = O, NH) and *cyclo*-$U_n(\mu_2$-X$)_n$ (n = 3, 4; X = C, CH, NH) clusters was verified by the magnetic criterion of aromaticity/antiaromaticity of a molecule, that of the nucleus-independent chemical shift, NICS(0), NICS(1), NICS(0), $NICS_{zz}(0)$ and the most refined $NICS_{zz}(1)$ index, along with the NICS scan profiles. All *cyclo*-U_nX_n (n = 3, 4; X = O, NH) and *cyclo*-$U_n(\mu_2$-X$)_n$ (n = 3, 4; X = C, CH, NH) clusters are predicted to be strongly aromatic molecules exhibiting high negative $NICS_{zz}(0)$ and $NICS_{zz}(1)$ values ranging from -135.2 to -359.9 ppm and from -40.1 to -170.6 ppm, respectively.

Finally, the E@[*cyclo*-$U_4(\mu_2$-C$)_4$], (E = H^+, C, Si, Ge) and U@[*cyclo*-$U_5(\mu_2$-C$)_5$] clusters keep to some extent the aromatic character of the respective metallacycle rings, which are quantified by the $NICS_{zz}(1)$ values in the range of -23.3 to -90.1 ppm. NBO analyses reveal significant electron transfer from the surrounding uranium atoms to the central ptE's, which acquire negative natural atomic charges and significantly increase the np_z ptE's orbital occupancies.